A Dynamic Target Tracking of Car-Like Wheeled Robot in a Sensor-Network Environment via Fuzzy Decentralized Sliding-Mode Grey Prediction Control

Chih-Lyang Hwang (clhwang@mail.tku.edu.tw), Tsai-Hsiang Wang, and Ching-Chang Wong
Department of Electrical Engineering, Tamkang University, Tamsui, Taiwan 25137, R.O.C.

Abstract— For implementing dynamic target tracking, two distributed CCD (charge-coupled device) cameras are set up to capture the poses of the tracking and target cars, which have the front-wheel for the steering orientation and the rear-wheel for the forward-backward motion. Based on the control authority of these two CCD cameras, a suitable reference command for the proposed controller of the tracking car is planned on a personal computer and then transmitted to the tracking car by a wireless device. Only the information of the upper bound of system knowledge is required to select the suitable scaling factors and coefficients of sliding surface for the proposed controller so that an acceptable performance is achieved. Since the target car is dynamic and the tracking car possesses dynamics, a grey prediction for the pose of the target car is employed to plan an effective reference command for the tracking car to enhance the performance of target tracking. Finally, a sequence of experiments is carried out to confirm the usefulness of the proposed control system.

Keywords: Senor-network environment, Target tracking, Car-like wheeled robot, Fuzzy sliding-mode control, Grey theory.

I. INTRODUCTION

Recently, distributed control applications within sensor networks are gaining a role of importance (e.g., [1]). Such senor-network environments are able to monitor what is occurring themselves, to build their own models, to communicate with their inhabitants, and to act on the basis of decisions they make. In a senor-network environment, many of the problems encountered by classic mobile robots (e.g., localization, different software for different mobile robot, sensor interference [2], and high computation power [3]) are solved.

The so-called intelligent environment is the objects inside of this space that can be detected by different CCDs. The area simultaneously observed by two CCDs is an overlapped region to completely monitor the interesting objects. In order to catch the synchronous image, a set of synchronizer can be installed. Based on the concept of "Senor-Network Environment", two distributed CCD cameras are employed to provide the pose of the tracking and target cars. After the image processing in a personal computer, the poses (i.e., position and orientation) of the tracking and target cars are applied to plan a reference command for the controller of the tracking car. This on-line planning trajectory is then transmitted to the tracking car by a wireless device.

Because the decentralized control scheme is free from the difficulties arising from the complexity in design,

debugging, data gathering, and storage requirements, it is more preferable for a tracking car than a centralized control. As one knows, a fuzzy control algorithm [4] consists of a set of heuristic decision rules and is regarded as a nonmathematical control algorithm, which has been proved to be very attractive whenever the controlled systems can't be well defined or modeled. In the beginning, a fuzzy decentralized sliding-mode control (FDSMC) for a tracking car is designed to control two unloaded motors [5]. One is for the steering angle, the other is for the angular (or forward-backward) velocity. Then a modification of scaling factor is employed to control the tracking car such that an acceptable performance of dynamic target tracking is achieved. The proposed control can track a reference command without the requirement of a mathematical model. Only the information of the upper bound of the tracking car is needed to choose suitable scaling factors and coefficients of sliding surface such that a satisfactory performance is obtained.

As one knows, a grey prediction is simple and effective. Because the target car is dynamic and the tracking car also possesses dynamics, a grey model is employed to predict the pose of target car [6]. Based on the predicted pose, a fuzzy decentralized sliding-mode grey prediction control (FDSMGPC) is designed such that an improved tracking result is obtained. Moreover, total eight tracking modes for target tracking are planned and executed by our car-like wheeled robots. The authors are supposed that these tracking modes can be a method for the problem of dynamic target tracking. Finally, a sequence of experiments in a sensor network environment is arranged to evaluate the effectiveness of the proposed control system.

II. SYSTEM DESCRIPTIONAND PROBLEM FORMULATION

A. System Description

Fig. 1 shows the block diagram of the overall system in senor-network environment. It includes a tracking car with a wireless device, a target car, two CCDs, and one personal computer, containing an image processing card and a wireless device. For a tracking car with size and shape, its location in the 2-D Cartesian space W can be uniquely determined by the spatial position (x, y) of the base point and the orientation angle θ with respect to the base point (see Fig. 2). The kinematics constraint of a nonholonomic tracking car is described as follows:

$$-\dot{x}(t)\sin\theta(t)+\dot{y}(t)\cos\theta(t)=0. \tag{1}$$

Furthermore, the velocity parameters of the tracking car are expressed as follows:

$$\dot{x}(t)=v\cos(\theta),\ \dot{y}(t)=v\sin(\theta),\ \text{and}\ \dot{\theta}(t)=v\tan(\phi)/l \tag{2}$$

where (x,y) denotes the position of the center of the tracking car, $\theta(t)$ is the angle between the orientation of the tracking car and the X-direction, ϕ is the orientation of the steering wheel with respect to the frame of the tracking car, v denotes the speed of the longitude (or rear-wheel), and l is the wheelbase of the tracking car. Similarly, the kinematics model of the front-wheel of the tracking car is the same as (2).

The photograph of the tracking car is depicted in Fig. 3. Except a wireless device, the target car is the same as tracking car. In this paper, the servo control system of the tracking car includes two DC motors, one digital signal processor (DSP), one driver, and one wireless device. The rear-wheels are fixed parallel to the car chassis and allowed to roll or spin but not slip; two front-wheels are parallel and can simultaneously turn to the right or left. Front-wheel and rear-wheel are individually driven by the same permanent magnet DC motor. The basic specifications of the tracking car are similar with [5].

The DC motor system is from Maxon Co. The DSP of TMS320LF2407 is from TI Co. The details can refer to our previous paper [5]. Because the proposed DSP does not have the interface of digital-to-analog converter (DAC), the corresponding circuit of 12-bits DAC (AD7541A) on the expansion circuit card is made by ourselves. In addition, it contains 16-bits decoder (HCTL2020). The wireless device SST-2450 is a spread spectrum radio modem with controlling an RS-232/RS-485 interface port. It is used for data acquisition and transmission between the personal computer and the tracking car. Its operating frequency range is between 2410.496 and 2471.936MHz. The channel spacing is 4.096MHz. Finally, the Matrox Meteor-II card is applied as an image processing card. It is a monochrome and component RGB analog frame grabber for standard and non-standard video acquisition. It is also available in a PCI or PC/104-Plus form factor, both of which can use a Matrox Meteor-II MJPEG module for compression and decompression of monochrome and color images. The software Matrox MIL-Lite 6.0 developed by Matrox possesses many modules, which can be used to recognize image.

B. Problem Formulation

The so-called intelligent environment is the objects inside of this space that can be detected by different CCDs. An overlapped region, simultaneously observed by two CCDs, is designed for completely monitoring the interesting objects. In order to catch the synchronous image, a set of synchronizer is installed. To distinguish the tracking car and the target car, two sets of three LEDs with different light area are respectively applied to the tracking car and the target car. Because the target car is dynamic and the tracking car possesses dynamics, a grey prediction for the pose of the target car is employed to plan an effective reference command for the tracking car to improve the tracking performance.

Finally, the main goal of this study is to investigate the tracking car using FDSMGPC for the target tracking in a sensor network environment. These experiments are categorized into the following three cases: (i) to track the target car moving with a curve "8" (without) using grey prediction, (ii) to track the same trajectory of part (i) using grey prediction for different initial time of the tracking car (e.g., two seconds delay), and (iii) to track the same trajectory of part (i) using grey prediction for different initial pose of the tracking car.

III. FUZZY DECENTRALIZED SLIDING-MODE GREY PREDICTION CONTROL

There are two subsections for the controller design of FDSMGPC.

A. Fuzzy Decentralized Sliding-Mode Control

Consider a tracking car with the following dynamic equation:

$$A(\sigma)\ddot{\sigma}(t)+B(\sigma,\dot{\sigma})+C(\sigma)+\Gamma(\sigma,\dot{\sigma},t)=DU(t) \tag{3}$$

where $\sigma(t)\in\Re^2$ is the angle of the tracking car, $A(\sigma)\in\Re^{2\times2}$ denotes the inertia matrix of positive definite for any $\sigma(t)$, $B(\sigma,\dot{\sigma})\in\Re^2$ comprises the centrifugal, Coriolis torques, $C(\sigma)\in\Re^2$ denotes the gravitational torque, $\Gamma(\sigma,\dot{\sigma},t)$ stands for the nonlinear time-varying uncertainties, $D\in\Re^{2\times2}$ represents a control gain, and $U(t)\in\Re^2$ is the control torque. It is assumed that the dynamics of (4) is unknown. However, the upper bound of function from (3) is supposed to be known.

The FDSMC includes two parallel FSMCs (cf. Fig. 4) with two sliding surfaces shown as follows:

$$S(t)=GE(t),\ G=\begin{bmatrix}G_1 & G_2\end{bmatrix},\ E(t)=\begin{bmatrix}E_1^T(t) & E_2^T(t)\end{bmatrix}^T \tag{4}$$

where $G_1=\text{diag}(g_{1ii})>0, G_2=\text{diag}(g_{2ii})>0\in\Re^{2\times2}, i=1,2$ are the scaling factors, $S(t)\in\Re^2$, and

$$E_1(t)=\sigma_r(t)-\sigma(t),\ E_2(t)=\dot{E}_1(t) \tag{5}$$

where $\sigma_r(t)=[\sigma_{r_1}(t)\ \sigma_{r_2}(t)]^T=[\phi_r(t)\ v_r(t)]^T\in\Re^2$ is a reference trajectory for the tracking car, $E_1(t)=[e_1(t)\ e_2(t)]^T$, and $E_2(t)=[e_3(t)\ e_4(t)]^T$. From (3) and (5), it leads to

$$\dot{E}_2(t)=\ddot{\sigma}_r(t)$$
$$-A^{-1}(\sigma)\big[DU(t)-B(\sigma,\dot{\sigma})-C(\sigma)-\Gamma(\sigma,\dot{\sigma},t)\big]. \tag{6}$$

The output of the FDSMC is designed as follows:

$$U(t)=G_3\hat{U}(t)=G_3\big[GE(t)+\Delta\,\text{sgn}(GE)\big]$$
$$=G_3\big[S(t)+\Delta\,\text{sgn}(S)\big] \tag{7}$$

where $G_3 = \text{diag}(g_{3ii}) > 0 \in \Re^{2\times2}$ is the output scaling factor, $\hat{U}(t)$ is fuzzy variable of $U(t)$, and $\Delta = \text{diag}(\delta_{ii}) > 0 \in \Re^{2\times2}$. Suppose that

$$g_{3ii} \geq \{a_m d_m [|f_i(t)| + \lambda_i]\}/(g_{2m}\delta_{ii}) \text{ for } i = 1,2 \quad (8)$$

where $\lambda_i > 0, g_{2m} = \lambda_{min}\{G_2\}, a_m = \lambda_{max}\{A(\theta)\}, d_m = \lambda_{max}\{D\}$, $f_i(t)$ is the ith element of the following matrix:

$$F(t) = G_1[\dot{\sigma}_r(t) - \dot{\sigma}(t)]$$
$$+ G_2\{\ddot{\sigma}_r(t) + A^{-1}(\sigma)[B(\sigma,\dot{\sigma}) + C(\sigma) + \Gamma(\sigma,\dot{\sigma},t)]\} \quad (9)$$

The following theorem discusses the fuzzy sliding-mode control for the partially unknown tracking car.

Theorem 1: Consider the unknown tracking car (3) with the known upper bound of (8), which is connected with the control parameters. Applying the control (7) with the satisfaction of condition (8) to the tracking car (3) gives the results (i) the finite time to reach the stable sliding surface (4), and (ii) the asymptotically tracking.

Proof: See [5] for a similar result.

Assume that $\dot{s}_i(t), i = 1,2$ increases as $u_i(t) = g_{3ii}\hat{u}_i(t)$ decreases; if $s_i(t) > 0$ then increasing $u_i(t)$ will result in decreasing $s_i(t)\dot{s}_i(t)$; and if $s_i(t) < 0$ then decreasing $u_i(t)$ will result in decreasing $s_i(t)\dot{s}_i(t)$. That is, the control input $u_i(t)$ is designed in an attempt to satisfy the inequality $s_i(t)\dot{s}_i(t) < 0$. To begin with, the fuzzy variable is quantized into the following seven qualitative fuzzy variables: (i) Positive Big (PB), (ii) Positive Medium (PM), (iii) Positive Small (PS), (iv) Zero (ZE), (v) Negative Small (NS), (vi) Negative Medium (NM), and (vii) Negative Big (NB). The inputs of fuzzy variable are defined as follows: $\hat{s}_i(t) = g_{iis}s_i(t)$ and $\dot{\hat{s}}_i(t) = g_{iis}\dot{s}_i(t)$, where $G_s = \text{diag}\{g_{11s}, g_{22s}\}$ and $G_{\dot{s}} = \text{diag}\{g_{11\dot{s}}, g_{22\dot{s}}\}$ are applied to normalize the values $\hat{s}_i(t)$ and $\dot{\hat{s}}_i(t)$ into the interval $[-1,1]$. There are many types of membership functions, some of which are bell shaped, trapezoidal shaped, and triangular shaped, etc. For brevity, the triangular type in Fig. 5 is used in this application. The linguistic rule of the ith FDSMC is achieved by the center of gravity method. Finally, a look-up table that directly relates the inputs $\hat{s}_i(t)$ and $\dot{\hat{s}}_i(t)$ with the output $\hat{u}_i(t)$ is also obtained (refer to our previous study for the detail). In summary, the control actions of the diagonal terms are ZE. This arrangement is similar to a variable structure controller that has a sliding surface. In addition, the control actions of the upper triangle terms are from PS to PB, and those of the lower triangle terms are from NS to NB. This fuzzy table is skew-symmetric (see [5]).

B. Grey Prediction

Prediction of the pose of target car is a common means for target tracking. The proposed method for the pose prediction is based on the grey theory [6], that assumes the internal structure, parameters, and characteristics of an observed system are unknown, or the so-called "black system." Based on the pose estimation of the target car by two CCDs, an appropriate model is assigned to approximate its dynamics. The approximate model is the so-called "white system." According to grey theory, the optimal parameters of the white system can be calculated. Generally, the grey model is written as $GM(\alpha, \beta)$, where α is the order and β is the number of variables of the modeling equation. The higher α is assigned, the more sensitive to the input data will the obtained model become. Among the GM family, the first-order one-variable grey model, i.e., GM(1,1), is most widely used and is successfully demonstrated in many applications such as forecasting, earthquake prediction, etc.

For tracking a dynamic target, the pose estimations from two CCDs is defined as $x(t)$, where t = 1, 2,…, n, and the accumulated generating operation is defined as the accumulated measurements $z(k) = \Sigma_{t=1}^k x(t)$ for (k = 1, 2,..., n). The dynamic change of z(t) is modeled by the following first-order ordinary differential equation:

$$dz(t)/dt + az(t) = b. \quad (10)$$

In grey theory, (10) is called the "white descriptor" for modeling a white system; the corresponding parameters a and b can be estimated from the poses of two CCDs. For effectiveness, equation (10) is approximated by the following grey-differential equation:

$$dz(t)/dt + ag(t) = b \quad (11)$$

where $g(t) = (z(t+1) + z(t))/2$. Then the least-square method is employed to obtain the optimal parameters by introducing the accumulated generating operation in a time interval. The first term of (11) in a discrete system can be written as

$$dz(t)/dt = z(t+1) - z(t) = x(t+1) \quad (12)$$

where the sampling time of measurements is taken as a unit. In addition, equation (11) can be rewritten as

$$x(t+1) = -0.5a[z(t+1) + z(t)] + b. \quad (13)$$

Substituting the sequential data x and z into (13) gives

$$\begin{bmatrix} x(2) \\ x(3) \\ \vdots \\ x(n) \end{bmatrix} = \begin{bmatrix} -0.5(z(2)+z(1)) & 1 \\ -0.5(z(3)+z(2)) & 1 \\ \vdots & \vdots \\ -0.5(z(n)+z(n-1)) & 1 \end{bmatrix} \begin{bmatrix} a \\ b \end{bmatrix} \quad (14)$$

or in a matrix form:

$$Y = B\Phi \quad (15)$$

where $Y = [x(2) \quad x(3) \quad \cdots \quad x(n)]^T$. For the case of $n \geq 2$, the following quadratic equation is defined for the cost function of least squares method.

$$J = (Y - B\Phi)^T(Y - B\Phi). \quad (16)$$

The optimal solution can be obtained by minimizing the J using the matrix derivation ∇ with respect to Φ as the following equations:

$$\nabla_\Phi J = 2[\nabla_\Phi(Y - B\Phi)^T][Y - B\Phi] \quad (17)$$

$$\nabla_\Phi(Y - B\Phi)^T = -\nabla_\Phi\Phi^T B^T = -B^T. \quad (18)$$

Setting (17) to zero, the optimal parameters of the grey model is obtained as follows:

$$\hat{\Phi} = \begin{bmatrix} \hat{a} & \hat{b} \end{bmatrix}^T = (B^T B)^{-1} B^T Y. \tag{19}$$

The estimated parameters are then brought into the response solution of the first-order ordinary differential equation (10) for the prediction of the accumulated generating operation:

$$\hat{z}(n+1) = \left[z(1) - \hat{b}/a \right] e^{-an} + \hat{b}/a. \tag{20}$$

Finally, the control block diagram of target tracking is depicted in Fig. 4. Different orders or variables of grey model can refer to some references, e.g., [7].

IV. EXPERIMENTS AND DISCUSSIONS

There are two subsections to discuss the experiments.

A. Experimental Preliminaries

1) Pose estimation

First, two sets of three LEDs with different light areas are placed to suitable locations of the tracking car and the target car, respectively. Then three corresponding points on the image plane to represent three positions with respect to the world coordinate (i.e., $(\hat{x}_1, \hat{y}_1), (\hat{x}_2, \hat{y}_2),$ and $(\hat{x}_3, \hat{y}_3)$ in Fig. 6) are obtained. Based on the relation (21), the world coordinate of the tracking car and the target car at geometry center is then attained.

$$\hat{\theta}(k) = \tan^{-1}\left\{\left[\hat{y}_1(k) - \left(\hat{y}_2(k) + \hat{y}_3(k)\right)/2\right]\right.$$
$$\left./\left[\hat{x}_1(k) - \left(\hat{x}_2(k) + \hat{x}_3(k)\right)/2\right]\right\} \tag{21}$$

$$\hat{x}(k) = \left(2\hat{x}_1(k) + \hat{x}_2(k) + \hat{x}_3(k)\right)/4 \tag{22}$$

$$\hat{y}(k) = \left(2\hat{y}_1(k) + \hat{y}_2(k) + \hat{y}_3(k)\right)/4. \tag{23}$$

The interpolation method is employed to obtain the relationship between the world coordinate and the image coordinate. This is a real world plane grabbed by CCD with the coordinate; the point (320,480) pixel on the image plane is defined as (0, 0) cm on the world coordinate. Fig. 7 shows the visible area by two CCDs, which possesses an overlapped region with width 24cm. The control authority in this overlap region is according to the distinguishable error; higher distinguishable error indicates higher control authority to monitor the tracking car or the target car. The maximum estimation error is about 2cm, which is acceptable and merely occurs in the periphery of the trapezoid. According to the restriction of grabbing frequency for a CCD, the sampling time for the image processing and trajectory planning is set as 130ms. While the tracking car or that target car is in the left trapezoid area, the related pose is estimated by CCD1. After trajectory planning, the reference command for the tracking car is sent by a wireless device. Similarly, as the tracking car or the target car is in the right trapezoid area, the corresponding pose is estimated by CCD2. When the tracking car or the target car is inside the overlap region, two CCDs can grab the image and the corresponding pose is estimated either by CCD1 or CCD2.

2) Strategy of target tracking modes

From the very beginning, various definitions for the strategy of target tracking are given in Fig. 8. These definitions are described as follows: (i) L_c (unit: cm) denotes the distance between the centers of the tracking car and target car, (ii) L_s (unit: cm) denotes the safe distance to avoid the bump of the target car by the tracking car, (iii) the point d represents the desired pose of the tracking car with a safe distance from the center of the target car and the same orientation of the target car, (iv) L_d (unit: cm) denotes the distance between the center of the tracking car and the point d, (v) θ_1 (unit: degree) denotes the angle between the orientation of the tracking car and the direction of the desired target pose with respect to the tracking car, and (vi) θ_2 (unit: degree) stands for the angle between the orientation of the tracking car and the direction of the tracking car with respect to the desired target pose. In addition, the tracking car and target car respectively depict in the color of dark blue and light blue. The angles for θ_1 and θ_2 are positive as it is in a counterclockwise direction. The normal velocity of the target car is assumed to be 1.2rps or $37.7\,\text{cm/s}$, which is about 60% of the highest velocity in this experiment. There are eight tracking modes in this study. Due to the symmetrical feature (i.e., the tracking car can be in the right-hand and left-hand sides of the target car), only 4 different modes (i.e., the tracking car is the left-hand side of the target car) are introduced as follows:

(1) The target car is in the front of the tracking car, and their orientation is consistent. It is so-called "tracking mode 1" (refer to Fig. 9). The numbers $1, 2, 3, \ldots$ with symbols square and circle represent the sequences of the tracking car and the target car, respectively. In this situation, the reference steering angle for the front-wheel (i.e., $\sigma_{r_1}(t)$ or $\phi_r(t)$) is set as follows (see Fig. 10(a)):

$$\sigma_{r_1}(t) = \begin{cases} -\theta_1, & \text{if } L_d > 10, \\ -\theta_2, & \text{otherwise,} \end{cases} \text{where} -30° \leq \theta_1, \theta_2 \leq 30°.$$

Simultaneously, the reference velocity for the rear-wheel (i.e., $\sigma_{r_2}(t)$ or $v_r(t)$) is assigned in Fig. 10(b) with $l_0 = 15\text{cm}, l_1 = 55\text{cm}, l_2 = 60\text{cm},$ and $l_3 = 100\text{cm}$.

(2) The target car is in the preceding of the tracking car, and their orientation is opposite. It is so-called "tracking mode 2" (see Fig. 11). The tracking car will be backward with the reference velocity -37.7 or -62.8cm/sec, which is inversely proportional to the distance L_c, and simultaneously turn right with the reference steering angle, e.g., $-30°$. After a few seconds, the reference velocity and the reference steering angle for the tracking car are simultaneously assigned 37.7cm/sec and 30 degree, respectively. Then the situation of the tracking and target cars is in the "tracking mode 1."

(3) The target car is at the back of the tracking car, and their orientation is consistent. It is so-called "tracking mode 3" (allude to Fig. 12). The tracking car will be forward with the reference velocity 37.7 or 62.8cm/s, which is

inversely proportional to the distance L_c , and simultaneously turn right with the reference steering angle, e.g., $-30°$. After a few seconds, $\sigma_{r_1}(t)$ and $\sigma_{r_2}(t)$ for the tracking car are simultaneously set as $30°$ and $-37.7 cm/sec$, respectively. Until the tracking car and the target are in the situation of "tracking mode 1", the sequential operation of the tracking car will follow the strategy of "tracking mode 1."

(4) The target car is at the back of the tracking car and their orientation is opposite. It is so-called "tracking mode 4" (see Fig.13). The tracking car will be backward with the reference velocity 37.7 or $62.8 cm/s$, which is inversely proportional to the distance L_c, and simultaneously turn right with the reference steering angle, e.g., $30°$. After a few seconds, $\sigma_{r_1}(t)$ and $\sigma_{r_2}(t)$ for the tracking car are respectively set as $30°$ and $-37.7 cm/sec$. Then the situation of the tracking and target cars is in the "tracking mode 1."

B. Experimental Results

Because the subsystem of steering angle is a type one system, its control input is the output of fuzzy table multiplied an output scaling factor g_{311}, i.e., an absolute control. On the contrary, the 2nd subsystem is a velocity control system, i.e., a type zero system. To eliminate the steady-state error of 2nd subsystem, an integrator is used for the output of fuzzy table multiplied an output scaling factor; i.e., 2nd subsystem is an incremental control system.

Due to the gear ratio of the steering subsystem is 190:1, the torque for driving the steering angle is enough. Hence, the scaling factors for this subsystem are the same as those in the unloaded tracking car. Because the 2nd subsystem is employed to drive the tracking car, the relative scaling factors are larger than those in the unloaded tracking car. In brief, $G_s = diag\{12.5, 1.2\}$, $G_{\dot{s}} = diag\{50, 300\}$, $G_3 = 6I_2$ are selected. Similarly, the sliding surface $G_1 = diag\{3125, 300\}$ and $G_2 = G_s$, has a larger value in the 2nd subsystem as compared with the unloaded case.

First, the target car moves with a curve of "8." Then the tracking car using FDSMC is employed to track the target car. The related response is shown in Fig. 14 (a), which is acceptable. At the same time, a FDSMGPC is applied for the above-mentioned case. For simplicity, only GM(1,1) grey model is applied to predict the pose of the target car. The corresponding response is presented in Fig. 14(b). Because the target car and the tracking car possess dynamics, a FDSMGPC indeed improves the system performance as compared with FDSMC. In fact, the faster motion of the target car moves, the predicted effect is more dominant. However, the target tracking is not merely the prediction problem. Faster motion of the target car will be difficult to track. Hence, a compromise should be made. In addition, different orders or variables for grey model can be considered to improve the prediction.

To verify the effectiveness, the target tracking of Fig. 14(b) case is verified by different initial time (e.g., two seconds delay as compared with Fig. 14(b)). The related response is shown in Fig. 15(a). Finally, the response of Fig. 14(b) case for different initial pose of the tracking car is depicted in Fig. 15(b). These responses are all in a satisfactory manner.

V. CONCLUSIONS

In sensor-network environment, many problems encountered by classic tracking cars are solved; e.g., localization, information about the environment, sensors, high computational power, different software, and sensor-based control for each tracking car are not required. The proposed control system included two processors (i.e., one DSP and one PC) with multiple sampling rates (i.e., 10ms and 130ms). Therefore, the bandwidth of the tracking car is still large enough to manipulate a high-frequency motion for dynamic target tracking. Furthermore, total eight tracking modes for target tracking are planned and executed by our car-like wheeled robots. The authors are supposed that these tracking modes can be a method for the problem of dynamic target tracking. The results of this paper can be extended to the number of the CCD camera greater than two.

REFERENCES

[1] T. Yamaguchi, E. Sato and Y. Takama, "Intelligent space and human centered robotics," IEEE Trans. Ind. Electron., vol. 50, no. 5, pp. 881-889, 2003.

[2] J. Minguez and L. Montano, "Nearness diagram (ND) navigation: collision avoidance in troublesome scenarios," IEEE Trans. Robot. & Automat., vol. 20, no. 1, pp. 45-59, 2004.

[3] R. C. Luo and T. M. Chen, "Autonomous mobile target tracking system based on grey fuzzy control algorithm," IEEE Trans. Ind. Electron., vol. 47, no. 4, pp. 920-931, 2000.

[4] T. H. S. Li and S. J. Chang, "Fuzzy target tracking control of autonomous mobile robots by using infrared sensors," IEEE Trans. Fuzzy Syst., vol. 12, no. 4, pp. 491-501, 2004.

[5] C. L. Hwang, L. J. Chang and Y. S. Yu, "Network-based fuzzy decentralized sliding-mode control for car-like mobile robots," IEEE Trans. Ind. Electron., Feb. 2007 (to be appeared).

[6] L. Jitao, W. Chengfa, X. Dasong, and L. Peigang, "Application of grey system theory to the forecasting and control of air environment quality," J. Grey Syst., vol. 4, pp. 181–192, 1992.

[7] T. L. Tien, "A research on the prediction of machine accuracy by the deterministic grey dynamic model DGDM(1,1,1)," Appli. Math. & Comp., vol. 161, pp. 923-945, 2005.
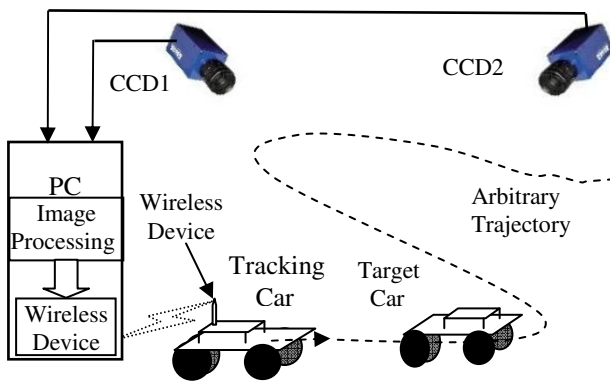
Fig. 1. The block diagram of the overall system.
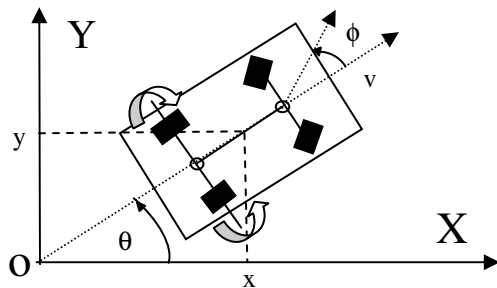
Fig. 2. Kinematic model of a tracking car.
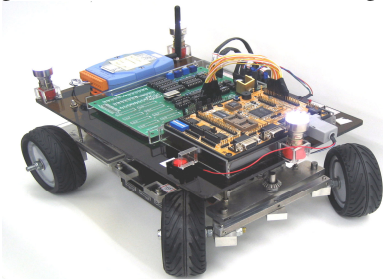
Fig. 3. Experimental setup of the tracking car.
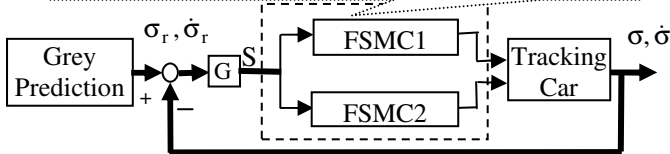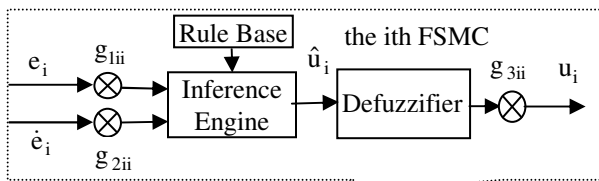
Fig. 4. Block diagram of FDSMGPC for the tracking car.
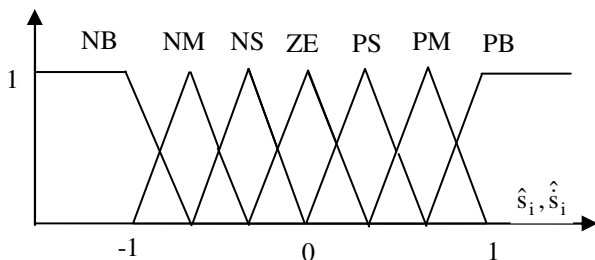
Fig. 5. Membership functions of triangular shape.
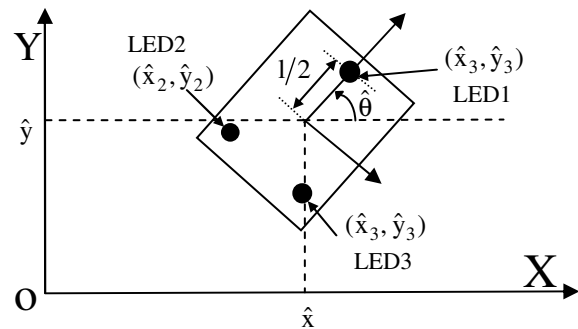
Fig. 6. The pose estimation of the tracking and target cars.
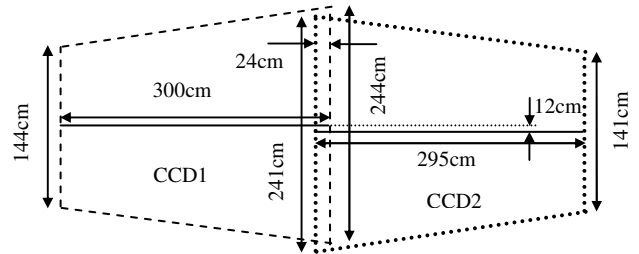
Fig. 7. The senor-network environment via two CCDs.
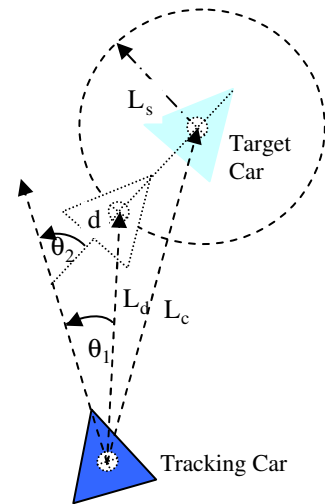
Fig. 8. Definitions for the strategy of target tracking.
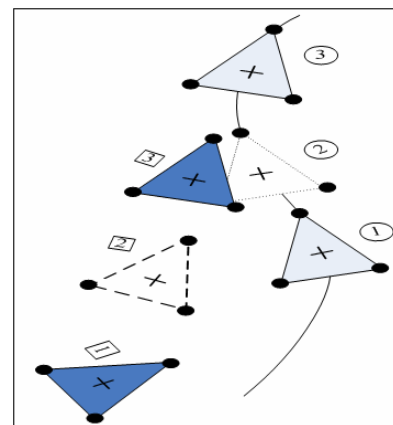
Fig. 9. Tracking mode 1.
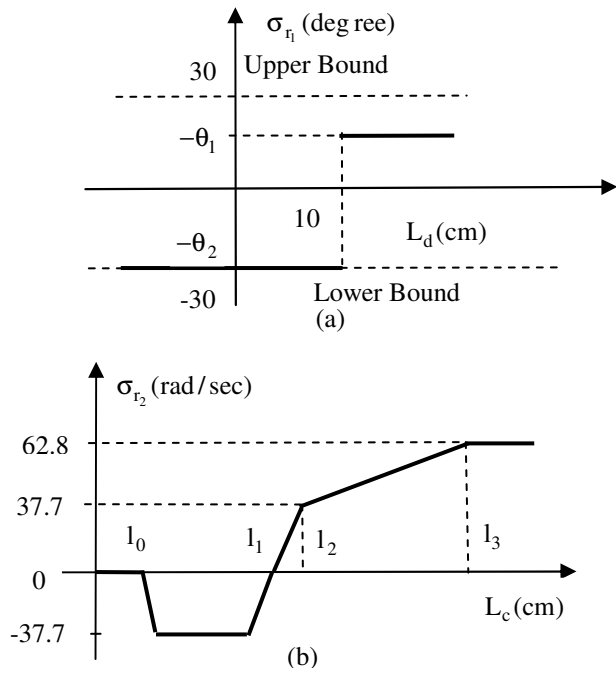
Fig. 10. The reference steering angle for the front-wheel and the reference velocity for the rear-wheel of tracking mode 1.
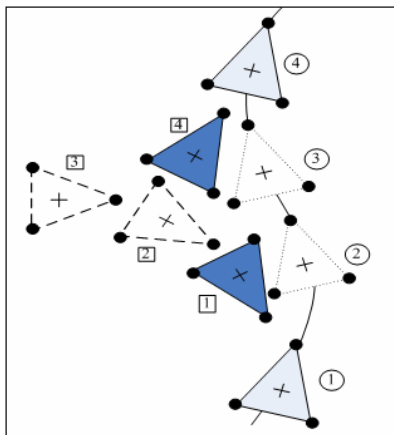
Fig. 11. Tracking mode 2.
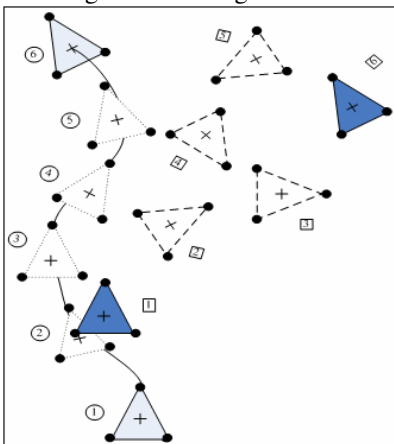
Fig. 12. Tracking mode 3.
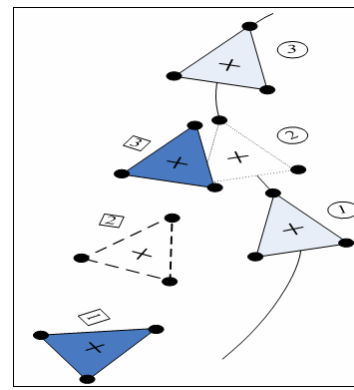
Fig. 13. Tracking mode 4.

(a)　　　　　　　　　　(b)
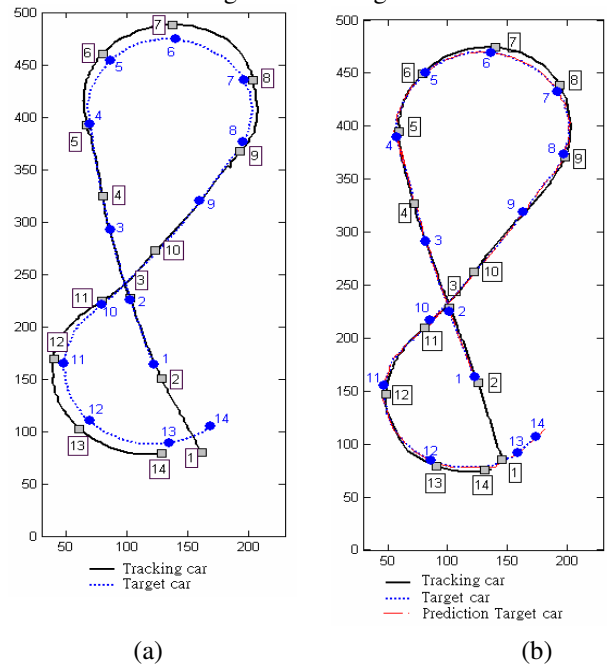
Fig.14. Experimental result of target tracking. (a) without using grey prediction. (b) using grey prediction.

(a)　　　　　　　　　　(b)
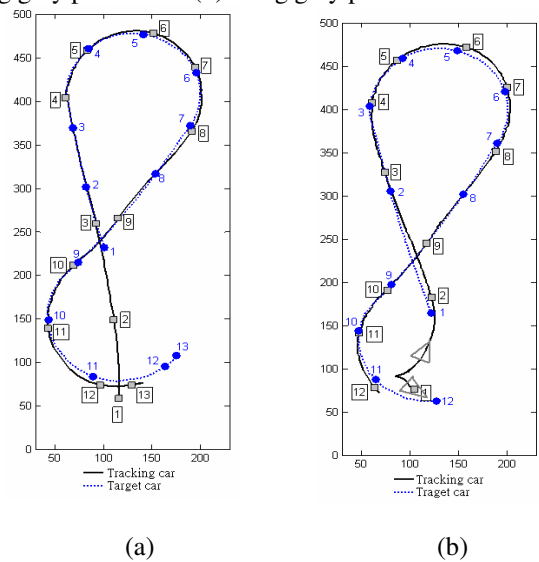
Fig. 15. (a) two seconds delay of tracking car for Figure 14(b) case, (b) different initial pose of tracking car for Figure 14(b) case.